European Journal of Pharmaceutics and Biopharmaceutics 74 (2010) 172–183

Contents lists available at ScienceDirect

European Journal of Pharmaceutics and Biopharmaceutics

journal homepage: www.elsevier.com/locate/ejpb

Research paper

Osmotically driven protein release from photo-cross-linked elastomers of poly(trimethylene carbonate) and poly(trimethylene carbonate-co-D,L-lactide)

R. Chapanian, B.G. Amsden *

Department of Chemical Engineering, Queen's University, Kingston, Ontario, Canada

ARTICLE INFO

Article history:
Received 29 April 2009
Accepted in revised form 23 November 2009
Available online 3 December 2009

Keywords:
Biodegradable elastomer
Protein delivery
Osmotic release
Mechanical properties

ABSTRACT

The potential of osmotic pressure driven release of proteins from poly(trimethylene carbonate) and poly(trimethylene carbonate-co-D,L-lactide) (poly(TMC-co-DLLA)) elastomers with varying amounts of DLLA was investigated using bovine serum albumin (BSA) as a model protein. The BSA was co-lyophilized with either trehalose or trehalose combined with NaCl as osmotigens to produce particles with sufficient osmotic activity. Elastomers composed solely of TMC were not suitable for osmotically driven release when trehalose was the main osmotigen in the solid particles. Copolymerizing TMC with small amounts of DLLA decreased the tear resistance of the elastomer and consequently increased the rate and the total amount of BSA released. Elongation at break played a significant role in determining the osmotic release behavior; elastomers with comparable Young's modulus and tensile strength, but smaller elongation at break, provided faster release rates. Elastomer degradation played a minor role in the osmotic release, as the mechanical properties underwent very little change during the investigated period of release. The poly(TMC-co-DLLA)(80:20) elastomer was able to provide near zero order release of BSA for up to 12 days, and the total amount of BSA released was 74 ± 4% after 34 days, when small amounts of NaCl was added to trehalose. No significant reduction in the microenvironmental pH occurred after 17 days of release. TMC elastomers copolymerized with small amounts of DLLA are potential candidates for the localized delivery of acid-sensitive proteins.

1. Introduction

The parenteral route remains the major route of protein administration [1]. Unfortunately, the pharmacokinetic half-life of many therapeutics proteins is short [2]. Thus, effective protein administration typically requires multiple injections, which are painful to the patient and costly to administer. Moreover, the resulting systemic exposure may produce undesired side effects. Conventional non-parenteral routes of administration suffer from problems related to slow protein transport through the epithelium and to degrading enzymatic activity at the site of administration [3]. Thus, there is increasing recognition within the pharmaceutical community for the importance of localized sustained delivery of proteins.

Protein therapeutics have been demonstrated to be released in a sustained and linear fashion from monolithic devices, when they are accompanied with osmotically active agents such as sugars and electrolytes [4–8]. The release is considered to occur in the following steps. Upon immersion in an aqueous media, water partitions into, then diffuses through, the polymer matrix. Upon encountering a polymer-surrounded drug particle (referred to as a capsule), the water dissolves the solid particle at the polymer/particle interface. The resulting saturated solution has a much lower water activity than the external solution, creating an enhanced water activity gradient. This activity gradient draws water into the capsule, generating a pressure equal to the osmotic pressure of the solution [9,10]. This pressure acts outwards on the polymer and is resisted by the viscoelastic nature of the polymer [1]. Two outcomes are possible [1,11]. If the pressure is sufficiently high, cracks are generated within the polymer. These cracks form a pore network that ultimately connects to the surface. The capsule contents are forced through the pore network as a result of the difference in pressure between the capsule and the external medium. If the pressure within the capsule is not high enough to generate cracks, the capsule remains swollen, and its contents are not released. This process repeats in a particle layer-by-particle layer manner until the centre of the device is reached. The mechanism can result in a constant release rate, depending on the geometry of the device; release is linear for slabs of much of the release period, and linear for cylinders until approximately 60% of the cumulative mass fraction is reached. For this osmotic pressure release process to be the principal release mechanism, the total volumetric loading of the solids within the polymer must be below the percolation threshold [2,12]. Other factors that control osmotically driven release rates include polymer physical properties and drug

* Corresponding author. Department of Chemical Engineering, Queen's University, Kingston, Ontario, Canada K7L 3N6. Tel.: +1 613 533 3093.
E-mail address: brian.amsden@chee.queensu.ca (B.G. Amsden).

0939-6411/$ - see front matter © 2009 Elsevier B.V. All rights reserved.
doi:10.1016/j.ejpb.2009.11.012

properties. Important polymer properties include hydraulic permeability, modulus, tensile strength and elongation at break. The principal drug properties include osmotic activity, water solubility, particle size, particle size distribution, volumetric loading, and homogeneity of dispersion throughout the polymer [1,6,11–14].

Recently, Gu et al. demonstrated the possibility of releasing proteins of different properties such as vascular endothelial growth factor (VEGF), interleukin-2 (IL-2) and interferon-γ (IFN-γ) from degradable elastomers synthesized from photo-cross-linked prepolymers of ω,ω,ω,-triacrylate [*star*-poly(ε-caprolactone-co-D,L-lactide)], via the osmotic release mechanism. In this case, the proteins were co-lyophilized with trehalose and bovine serum albumin (BSA) [8,15]. The device was able to provide a constant release for 5–20 days, depending on the device geometry, solid particle composition and elastomer cross-link density [7,15,16]. Unfortunately, these elastomers degrade by hydrolysis to yield acidic products that decreased the microenvironmental pH within the device. This pH decrease has been implicated in the denaturation of acid labile proteins such as VEGF, *in vitro*, after 7–10 days [8,15].

Since polymers made of trimethylene carbonate (TMC) degrade without producing acidic products [17–19], we hypothesized that TMC-based elastomers would be capable of releasing proteins via the osmotic release mechanism without an accompanying pH decrease in the device. To explore this hypothesis, BSA was used as a model protein. BSA was lyophilized with trehalose and a mixture of trehalose and sodium chloride (NaCl) as osmotigens and incorporated as solid particles into TMC-based elastomers. The effect of the mechanical properties of the TMC-based elastomers on the release of BSA was investigated by copolymerizing TMC with different amounts of D,L-lactide (DLLA). The *in vitro* degradation of these elastomers was followed by measuring the changes in their mechanical properties, sol content, water uptake, and weight loss of the elastomers, and through measurements of their surface chemistry using attenuated total reflectance-FTIR (ATR-FTIR) spectroscopy. Fluorescein isothiocyanate labeled BSA (FITC-BSA) was used to track the *in vitro* release of protein particles from the elastomer and to assess the microenvironmental pH within the elastomer during release.

2. Materials and methods

D,L-Lactide (DLLA) (99+%) was obtained from Purac, the Netherlands, and purified by recrystallization from dried toluene. 1,3-Trimethylene carbonate (1,3-dioxan-2-one) was obtained from Boehringer Ingelheim, Germany, and used as received. Toluene and dichloromethane were dried over calcium hydride and distilled under argon. Other chemicals were used without further purification. Chemicals used in polymer synthesis include stannous 2-ethylhexanoate (96%) obtained from Aldrich, Canada, and glycerol obtained from BDH, USA. Chemicals used in the acrylation process include acryloyl chloride (96%), triethylamine (99.5%) and 4-dimethylaminopyridine (99%), all obtained from Aldrich, Canada. 2,2-Dimethoxy-2-phenylacetophenone used as a photoinitiator was obtained from Aldrich, Canada. Solvents used for purification of the synthesized polymers include ethyl acetate (99.9%), and methanol (99.8%), and were obtained from Fisher, Canada. For the release studies, trehalose, bovine serum albumin (BSA) and NaCl were all obtained from Sigma, Canada. Chemicals used in calorimetric assays include Coomassie brilliant blue G obtained from Fluka, Canada, and phosphoric acid (85%) and sulfuric acid (95–98%) obtained from Fisher, Canada.

2.1. Preparation of solid particles

BSA was reconstituted with trehalose or a mixture of trehalose and NaCl in 5 mM pH 7 succinate buffer with a final concentration of 400 mg in 10 mL of buffer. Reconstituted solutions were frozen in liquid nitrogen and lyophilized on a Modulyo D freeze-dryer (Thermosavant, USA) at 100 μbar for 2 days. The lyophilized powder was ground using a mortar and pestle and sieved through a Tyler 60 sieve to yield particles less than 250 μm in diameter. Reconstituted protein solutions were composed of either 10 w/v% BSA, 90 w/v% trehalose, or 10 w/v% BSA, 25 w/v% NaCl, 65 w/v% trehalose.

2.2. Prepolymer preparation

ω,ω,ω-Triacrylate [*star*-poly(TMC)] and [*star*-poly(TMC-co-DLLA)] of theoretical molecular weights of 7800 Da and with DLLA content of 5%, 20% and 50% by mole were prepared by ring-opening polymerization initiated with glycerol and catalyzed with stannous(II) ethylhexanoate at 130 °C for 72 h, as described previously [20]. For acrylation, warm star-copolymer was poured into a dried round-bottom flask, the flask was sealed with a rubber septum and then purged with dry argon. The following procedures were conducted in a glove box. Dried dichloromethane was added to the flask at a ratio of polymer to solvent of 2:1 (w:v) to dissolve the polymer. Triethylamine was added at a molar ratio of 1 mol per mole of star-copolymer (SCP) hydroxyl group, while the 4-dimethylaminopyridine catalyst was added at a molar ratio of 2×10^{-3} mole per mole of SCP terminal hydroxyl group. Finally, acryloyl chloride was diluted in dried dichloromethane at a ratio of 1:1 (v:v) and added slowly in a drop-wise fashion at a ratio of 1.2 mol per mole of SCP hydroxyl group. For ^{1}H NMR analyses, the SCP and acrylated star-copolymer (ASCP) were dissolved in dimethyl sulfoxide-d_6 (DMSO-d_6), and the spectra were acquired using a 500 MHz Bruker-Avance spectrometer. The chemical structure of the poly(TMC-co-DLLA) copolymer before and after acrylation is presented in Fig. 1A.

2.3. Elastomeric rod preparation

To prepare elastomeric rods, prepolymer of a given composition was dissolved in ethyl acetate at a ratio of 1:1 (w:w) and 1.5 w/w(polymer)% of 2,2-dimethoxy-2-phenylacetophenone was added as a photoinitiator. A previous optimization study indicated that this initiator concentration was sufficient to produce elastomers with low sol contents [21]. The mixture was poured into glass tubes sealed at one end, then closed with a rubber septum at the other end. The tube was connected to the shaft of a motor, rotated at 200 rpm and exposed to long-wave UV light (320–480 nm) at an intensity of 40 mW/cm^2 for 2 min using an EXFO E3000 light source. The purpose of rotating the samples, while being exposed to UV light, was to provide a homogenous exposure to UV radiation. The rubber septum was removed, and the glass was cut from the sealed side to facilitate the evaporation of ethyl acetate. Samples were left in the fumehood overnight and then exposed to vacuum for 48 h. The elastomer rods were gently removed from the glass tubes, and the sol was extracted using dichloromethane. The density of the elastomers was measured using the volume displacement technique according to ASTM D792-08, where absolute ethanol was used as the displacing liquid.

2.4. In vitro degradation

The *in vitro* degradation of the elastomers was performed in pH 7.4 phosphate-buffered saline. The pH of the buffer was maintained by replacing the buffer once every week. The degradation process was followed by measuring mechanical properties, water uptake, sol content, mass loss and surface chemistry of the elastomer samples. At time points of 1, 4, 12, 18, 24, 30 and 40 weeks, five rods were removed from the buffer, washed with distilled water, blotted dry, and their wet weight (w_w) was measured. Four rods in their wet state were used to determine the mechanical

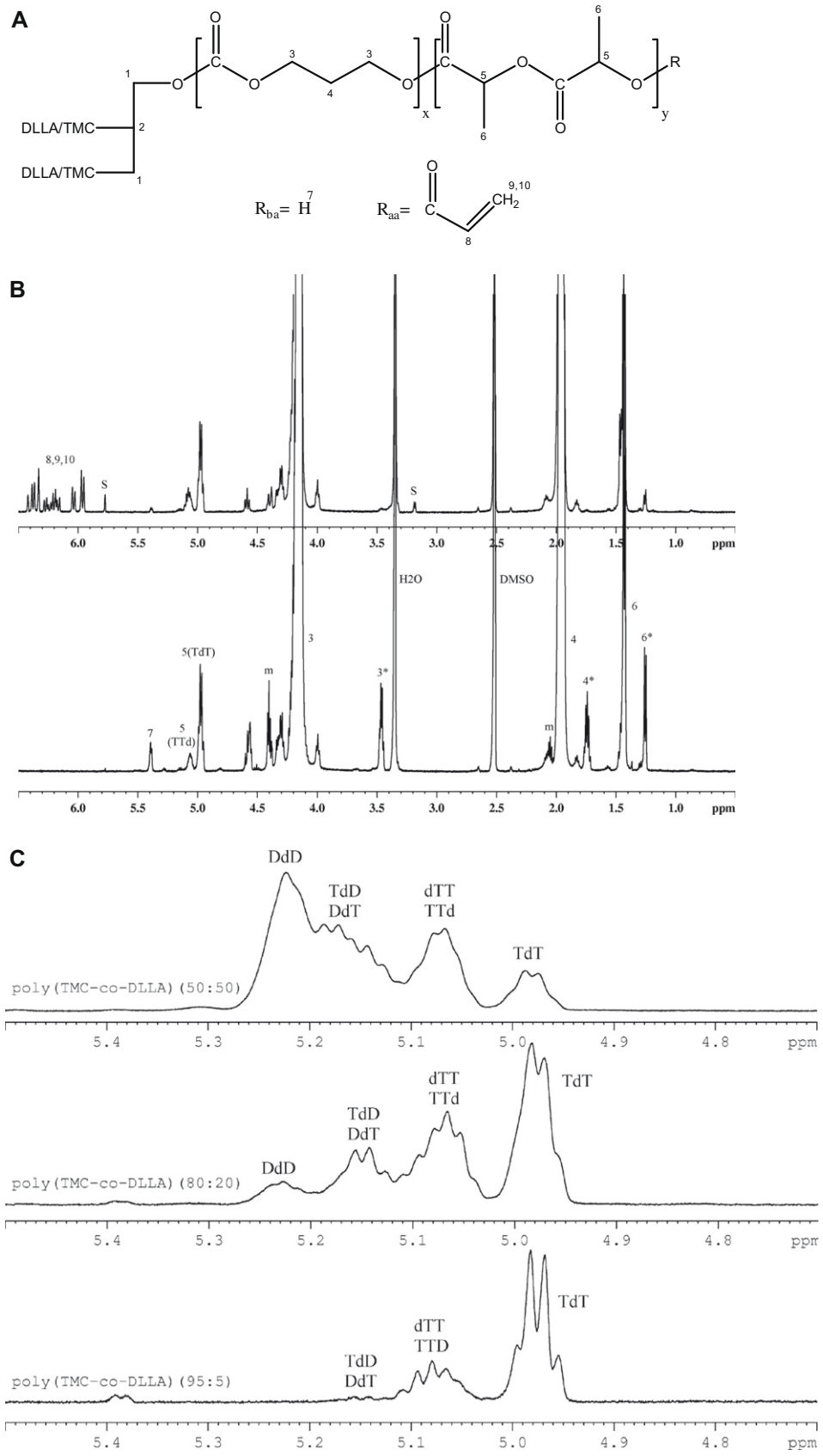

Fig. 1. (A) The chemical structure of poly(TMC-co-DLLA); the subscript ba refers to before acrylation, while aa refers to after acrylation. The numbers indicate the corresponding protons in the structure of the copolymer. (B) ^{1}H NMR spectra of poly(TMC-co-DLLA)(95:5), before acrylation (bottom) and after acrylation (top); m = monomer, s = solvent, ∗ indicates the chemical shift of the corresponding proton on the end group. (C) ^{1}H NMR spectrum of methine group of lactyl units in poly(TMC-co-DLLA) with different molar composition of DLLA; DdD = lactyl unit surrounded by two lactyl units, DdT = lactyl unit surrounded by one lactyl and one carbonyl unit, TTd = carbonyl unit surrounded by one carbonyl and one lactyl units and TdT = lactyl unit surrounded by two carbonyl units.

properties, measured using an Instron uniaxial tensile tester model 4443. The cross-head speed was set at 500 mm/min according to ASTM D412. All specimens were tested at room temperature. Data analysis was carried out using a Merlin 4.11 Series IX software package. To determine dry weight (w_d), samples used for mechanical testing were dried in a vacuum oven at 45 °C for 3 days. The water uptake was calculated using the following equation:

$$\text{Water uptake } (\%) = \frac{w_w - w_d}{w_d} \times 100 \quad (1)$$

Mass loss was calculated using the following equation:

$$\text{Mass loss } (\%) = \frac{w_0 - w_d}{w_0} \times 100 \quad (2)$$

in which w_0 is the initial weight of the sample before implantation. In order to determine sol content, dried samples were immersed in 3 mL dichloromethane per rod. The dichloromethane was replaced three times at 2 h intervals, after which the samples were dried at 45 °C under vacuum for 3 days. The sol content was calculated using the following equation:

$$\text{Sol content } (\%) = \frac{w_d - w_e}{w_d} \times 100 \quad (3)$$

in which w_e is the weight of the sample after sol extraction. Water uptake, mass loss and sol content were determined from triplicate samples unless otherwise mentioned. The fifth rod was used to investigate the chemical structural alteration during degradation via ATR-FTIR analyses, performed using a Nicolet Avatar 320 FTIR with a golden gate. A single pass diamond attenuated total reflectance attachment was employed, operating with 64 scans and at a resolution of 4 cm^{-1}. The data were analyzed using GRAMS/32 AI(32) (6) software. The thermal properties of the prepolymers and elastomers were measured using Mettler Toledo DSC 1 STAR^e system. Samples with a weight of 4–6 mg were subjected to heating–cooling–heating cycles after cooling them to −80 °C at first. The rate of heating and cooling was set at 5 °C/min.

2.5. Device preparation

Sieved BSA-containing particles were added to 1:1 (w:w) prepolymer solution of ethyl acetate containing 1.5 w/w(polymer)% of 2,2-dimethoxy-2-phenylacetophenone as photoinitiator, and the mixture was homogenized by gently mixing with a spatula. The suspension was filled into a glass tube and cross-linked with rotation as described earlier. The resulting particle-filled, elastomer rods were gently removed from the glass tubes, the solvent was evaporated, and their dimensions and weight were recorded. Each rod was then placed in an Eppendorf tube with 1 mL sterile pH 7.4 phosphate-buffered saline (PBS) containing 0.2 w/v% sodium azide. The PBS buffer was replaced frequently to approximate infinite sink conditions, and at each time point, the rods were removed, blotted dry and weighed to determine the water uptake. The water uptake was calculated using Eq. (1), in which w_d was determined by subtracting the mass of particle released from the initial mass of the device. The amount of BSA in the release media was measured using a Bradford micro-assay [22]. Briefly, 150 μL of release media was added in duplicate in the wells of a 96-well plate. Bradford solution with the volume of 150 μL was then added using a multichannel pipette, the plate was located on a plate mixer for 1 min, then left for 10 min on the bench, and the color change was recorded at 595 nm using a μQuant Universal Microplate Spectrophotometer model H1034 from Bio-Tek Instruments Inc. Quantification of released trehalose was performed using phenol–sulfuric acid calorimetric assay as follows [23]. Twenty microliters of 80% phenol in distilled water was added to 0.4 mL of released media, gently mixed, and 1 mL of concentrated sulfuric acid was added, the stream of acid being directed against the liquid surface. After 10 min, the liquid was vortexed and left for 20 min at 30 °C, after which 300 μL was located in duplicate in a 96-well plate, and the reading was taken at 480 nm.

2.6. Statistics

All data are presented as the mean ± the standard deviation about the mean unless otherwise mentioned. Where indicated, pair-wise comparisons were performed using a one-way ANOVA with a Tukey post hoc analysis. Paired comparisons were considered significantly different for $p < 0.05$.

3. Results and discussion

3.1. Prepolymer composition

The DLLA content in the star-copolymers was determined from the relative area under the chemical shifts corresponding to H_6 and H_{6^*} of DLLA and H_4 of TMC from the ^{1}H NMR spectra of the ASCP (Fig. 1B); the results were listed in Table 1. The DLLA content in the star-copolymers was very close to the feed ratio, indicating nearly complete consumption of the DLLA during the polymerization. At low-DLLA composition, most of the TMC monomer reacted as well, with less than 2% unreacted in poly(TMC), poly(TMC-co-DLLA)(95:5) and poly(TMC-co-DLLA)(80:20). However, with 50 mol% DLLA in the feed, 13% of the TMC remained unreacted (Table 1). The amount of unreacted TMC was calculated from the area of the –$CH_2CH_2CH_2$– monomer peak at 2.05 ppm (m) relative to the area of the peaks corresponding to H_4 and H_{4^*} in the polymer, using the ^{1}H NMR spectra of the SCP (Fig. 1B). The higher amount of unreacted TMC monomer in poly(TMC-co-DLLA)(50:50) is attributed to the lower reactivity of TMC [24].

^{1}H NMR analysis of poly(TMC-co-DLLA)(95:5) showed two methine signals, one at 4.98 ppm for non-terminal lactyl units and one at 5.09 for terminal lactyl units (Fig. 1B). Using the relative areas of peaks corresponding to the end groups (H_7 of hydroxyl group of DLLA and H_{3^*} of methylene group of TMC), it was determined that in the copolymers, the chains were predominantly terminated with lactyl units. In poly(TMC-co-DLLA)(95:5), for example, the amount of terminal lactyl was 34.3% compared to 72.1% in the case of poly(TMC-co-DLLA)(80:20) (Table 1). The accumulation of lactyl units at the end was due to transesterification, since the primary hydroxyl groups derived from TMC units are more reactive in transesterification, and consequently they become depleted [25]. A low amount of

Table 1
Chemical and physical properties of synthesized prepolymers, determined from ^{1}H NMR analyses.

Prepolymer	DLLA content (mol%)	Terminal DLLA (mol%)	Unreacted TMC (mol%)	DA (%)	M_n (kDa)
TMC	–	–	<2%	75.4	8.6
TMCDLLA(95:5)	4.9	34.3	<1%	86.7	8.5
TMCDLLA(80:20)	20.2	72.1	<1%	85.2	8.3
TMCDLLA(50:50)	53.9	73.1	13%	89.3	7.8

DA: degree of acrylation. M_n was determined from ^{1}H NMR using end-group analysis of acrylate groups and remaining unreacted end groups.

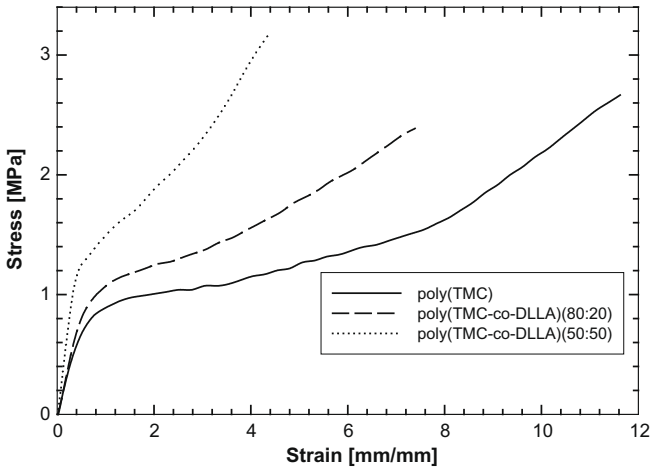

Fig. 2. Representative stress–strain curves of poly(TMC) and poly(TMC-co-DLLA) elastomers.

DLLA in the structure of the copolymer produced shorter DLLA blocks (Fig. 1C). The average lactyl sequence length, $\bar{L}_{LA}$, was calculated using integrations of representative methine groups of lactyl units in the 4.9–5.3 ppm region and the following equation [26,27]:

$$\bar{L}_{LA} = \frac{1}{P_{L\to T}} = \frac{1}{P_{T\to L}} = \frac{DdD + (DdT + TdD) + (TTd + dTT) + TdT}{DdT + TTd + TdT} \quad (4)$$

where $P_{L\to T}$ is the probability of a lactyl unit being beside a carbonyl unit from the left to right direction, and the lower case (d) indicates a lactyl unit surrounded by two other lactyl units (D). Determination of $\bar{L}_{LA}$ was performed with some approximation because of the incomplete separation of the corresponding peaks. In poly(TMC-co-DLLA)(50:50), the average lactyl unit sequence length $\bar{L}_{LA}$ was 2.8 compared to 1.49 in poly(TMC-co-DLLA)(80:20). These values are similar to those reported by Pego et al. [28] and indicate that the 80:20 star-copolymer has single lactyl units connected to TMC on either side. This chemical sequence occurs due to transesterification reactions during the polymerization.

The degree of acrylation was calculated from the ^{1}H NMR spectra of purified ASCP by end-group analysis using the relative areas of end-group peaks (H_{10}, H_{6^*}, and H_{3^*}). The degree of acrylation increased with increasing DLLA content in the prepolymer, ranging from 75.4% for poly(TMC) to 89.3% for poly(TMC-co-DLLA)(50:50) (Table 1). A significant decrease in hydroxyl peaks of terminal lactyl units at δ = 5.42 ppm (H_7) and terminal methylene groups of carbonyl units at 1.75 ppm (H_{4^*}) and 3.47 ppm (H_{3^*}) and terminal methyl groups of lactyl units at 1.26 ppm (H_{6^*}) were observed after acrylation (Fig. 1B). Using end-group analysis, the number average molecular weight (M_n) of the star-copolymers was found to be very close to the theoretical molecular weight of 7800 Da (Table 1).

3.2. Elastomer properties

Copolymerizing TMC with DLLA of up to 20 mol% did not change the stiffness of the elastomer (Fig. 2). Poly(TMC), poly(TMC-co-DLLA)(95:5) and poly(TMC-co-DLLA)(80:20) elastomers had roughly equal Young's moduli of 1.8 ± 0.1 MPa, and the stress at break (σ_b) values of those elastomers were also not significantly different (Table 2). The σ_b value of the poly(TMC-co-DLLA)(95:5) elastomer was 2.6 ± 0.1 MPa and that of poly(TMC-co-DLLA)(80:20) elastomer was 2.5 ± 0.1 MPa. The greatest σ_b value recorded for poly(TMC) elastomer was 2.6 MPa, and this was due to the slippage of elastomer samples from the grips of the tensile tester. Further addition of DLLA produced a stiffer elastomer; poly(TMC-co-DLLA)(50:50) had a Young's modulus of 3.3 ± 0.2 MPa, which was 1.8 times greater than the modulus of poly(TMC) and poly(TMC-co-DLLA) with DLLA contents of 5% and 20%. On the other hand, poly(TMC-co-DLLA)(50:50) had 1.3 times the σ_b as the other copolymers. Poly(TMC-co-DLLA)(50:50) had a σ_b of 3.2 ± 0.4 MPa, compared to 2.5 ± 0.1 MPa for poly(TMC-co-DLLA)(80:20) and 2.6 ± 0.1 MPa to poly(TMC-co-DLLA)(95:5). Addition of DLLA to the elastomers had a marked effect on the strain at break (ε_b). Adding only 5 mol% DLLA reduced the ε_b 1.4 times, while further addition of DLLA decreased ε_b 1.8 times in poly(TMC-co-DLLA)(80:20) and 2.7 times for poly(TMC-co-DLLA)(50:50).

The elastomers were amorphous and rubbery at 37 °C (Table 3). The glass transition temperature increased with the increase in DLLA content, being −14.1 °C for the TMC elastomer, and increas-

Table 2
Physical and mechanical properties of synthesized elastomers.

Elastomer	Sol content (%)	d (g cm^{-3})	E (MPa)	σ_b (MPa)	ε_b (mm/mm)
TMC	28.1 ± 0.5	1.357	1.8 ± 0.1	>2.6	>12.9
TMCDLLA(95:5)	21.1 ± 0.5	1.333	1.8 ± 0.1	2.6 ± 0.1	9.4 ± 0.4
TMCDLLA(80:20)	20.3 ± 0.4	1.281	1.8 ± 0.1	2.5 ± 0.1	7.3 ± 0.4
TMCDLLA(50:50)	12.7 ± 0.6	1.270	3.3 ± 0.2	3.2 ± 0.4	4.7 ± 0.4

E: Young's modulus; d: density; σ_b: stress at break and ε_b: elongation at break. The mechanical properties were determined from sol removed elastomers, and the network density is for non-sol removed elastomers.

Table 3
Thermal properties of prepolymers and sol removed elastomers in dry and hydrated states.

	ASP	Dry elastomer		Hydrated elastomer				
	T_g (°C)	T_g (°C)	T_m (°C)	T_g (°C)	T_{m1} (°C)	T_{m2} (°C)	DH_1 (J/g)	DH_2 (J/g)
TMC	−20.4	−14.1	–	−17.7	1.1	83	3.1	23.1
TMCDLLA(95:5)	−18.1	−12.3	–	−14.5	1.2	86	1.6	15.4
TMCDLLA(80:20)	−11.1	−4.2	–	−6.2	1.2	77	1.6	13.5
TMCDLLA(50:50)	6.4	13.2	–	N/A	1.7	92	N/A	10.85

ASP: acrylated star prepolymer, T_{m1} and ΔH_1: melting point and enthalpy due to the presence of free water in the elastomer, T_{m2} and ΔH_2: melting point and enthalpy due to the interaction of water molecules with polymer molecules. N/A: properties that were not determined due to the coexistence of the glass transition and melting endotherm at the same region. The properties of ASP and dry elastomer were determined from the second heating cycle, whereas the properties of the hydrated elastomer were determined from the first heating cycle.

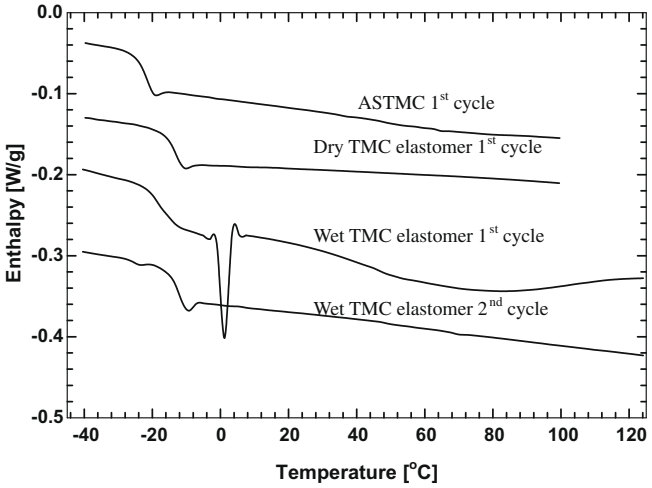

Fig. 3. Differential scanning calorimetry thermogram of TMC prepolymer and dry and hydrated elastomers. ASTMC: acrylated star TMC.

ing to 5.2 °C in poly(TMC-co-DLLA)(50:50) (Table 3). The glass transition temperature of the elastomers was greater than the glass transition temperature of their corresponding prepolymers (Table 3), due to the restricted mobility of polymer chains in the elastomer arising as a result of cross-linking. The glass transition temperature of the elastomers in the wet state was slightly lower than that of the dry state (Table 3), due to the plasticizing effect of water molecules. Furthermore, the hydrated elastomers exhibited two endotherms: a sharp endotherm near 0 °C, corresponding to the melting of free water in the elastomer and a broad endotherm, at around 80 °C, corresponding to the interaction of water molecules with elastomer network chains. The magnitude of the two endotherms was the greatest in the TMC elastomer, and it decreased with increasing DLLA content in the elastomer (Table 3). The endotherms were present only in the first heating cycle. The enthalpies and glass transition temperature of the hydrated elastomers are also listed in Table 3. Albertsson and Eklund have reported that although linear PTMC with average molecular weights of 57 and 75 kDa was amorphous, linear PTMC with an average molecular weight of 4600 Da was semi-crystalline with a melting point of around 35 °C [29]. Furthermore, upon exposure to PBS at 37 °C, a second melting point was formed at around 52 °C. In contrast, the star-PTMC in this study was unable to crystallize (Fig. 3).

3.3. Efficiency of photocuring

The increased degree of acrylation with increasing DLLA content in the elastomer resulted in elastomers with a lower sol content (Table 2), indicative of a more efficient cross-linking reaction. The efficiency of the photocuring process was also investigated using ATR-FTIR analyses. Upon acrylation of poly(TMC-co-DLLA)(80:20), a new band was formed at 1630 cm^{-1}, which was assigned to the C=C stretching (Fig. 4A and B). After photocuring, the newly formed band disappeared, indicating the consumption of the double bond (Fig. 4B). In a previous study, we found that the C=C stretching band in a poly(DLLA-co-ε-CL) elastomer made of a prepolymer of an average molecular weight of 1250 Da was totally consumed at a depth of 1 mm, also indicating a high photocuring efficiency [30].

3.4. BSA release

The volumetric loading in our experiments was kept below the percolation threshold to minimize the contribution of diffusion

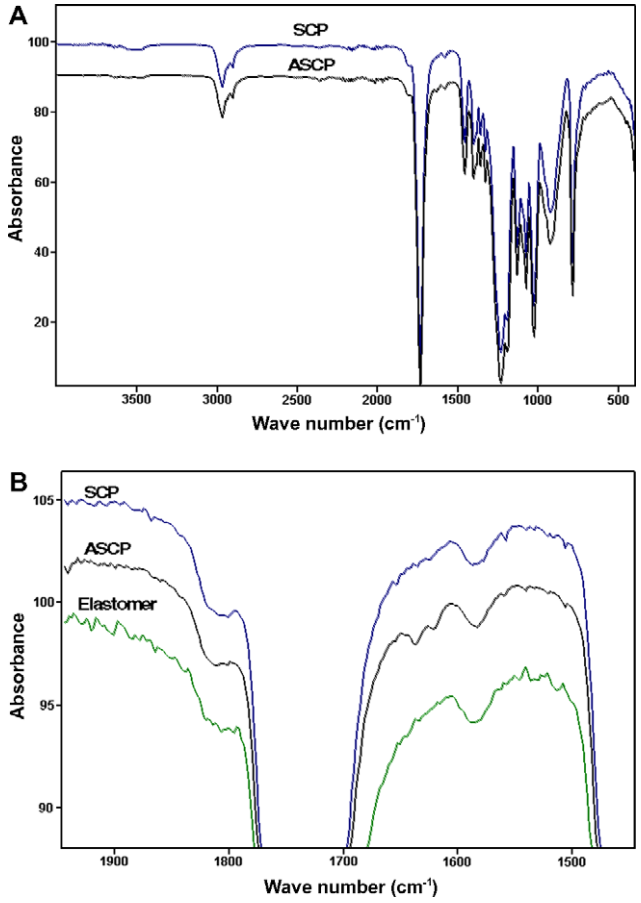

Fig. 4. ATR-FTIR analyses of synthesized poly(TMC-co-DLLA)(80:20) prepolymer and elastomer. (A) Prepolymer spectrum before and after acrylation. SCP: star-copolymer and ASCP: acrylated star-copolymer. (B) C=C stretch region of SCP, ASCP and the elastomer. (For interpretation to colours in this figure, the reader is referred to the web version of this paper.)

and thus to obtain an effective osmotic release mechanism [2,12]. To form solid particles with an appreciable osmotic activity, BSA was co-lyophilized with trehalose, which is known to be an effective lyoprotectant and a compatible osmolyte that accumulates in organisms under stress conditions [31]. A saturated solution of trehalose can provide an osmotic pressure of 92 atm at 37 °C [32].

Although trehalose was capable of generating effective BSA release from ε-caprolactone-D,L-lactide-based elastomers [7,15], trehalose was unable to generate significant BSA release from the TMC elastomer (Fig. 5A). Moreover, these rods continued to draw in water and to swell for up to 40 days in PBS buffer (Fig. 5B). Thus, it appears that elastomers composed solely of TMC are not suitable for osmotically driven release when trehalose is the main osmotically active component.

Osmotic release is driven not only by the osmotic pressure of the solution generated within the capsule, but also by the mechanical properties of the elastomer [11,13], which have been shown earlier in this article to be influenced by the amount of DLLA incorporated into the polymer. For these elastomers, the release occurred in two phases. The first phase appeared to be primarily diffusionally controlled, releasing a total mass fraction of consistently approximately 6 ± 2%. During this phase, BSA particles near the surface were released by dissolution and diffusion. This was followed by a second release phase, due to the osmotic release mechanism. The release rate was faster, and larger mass fractions of BSA were released, when the DLLA of the elastomer was increased. For example, at day 38, elastomers made of poly(TMC-co-DLLA)(50:50) released a cumulative mass fraction of

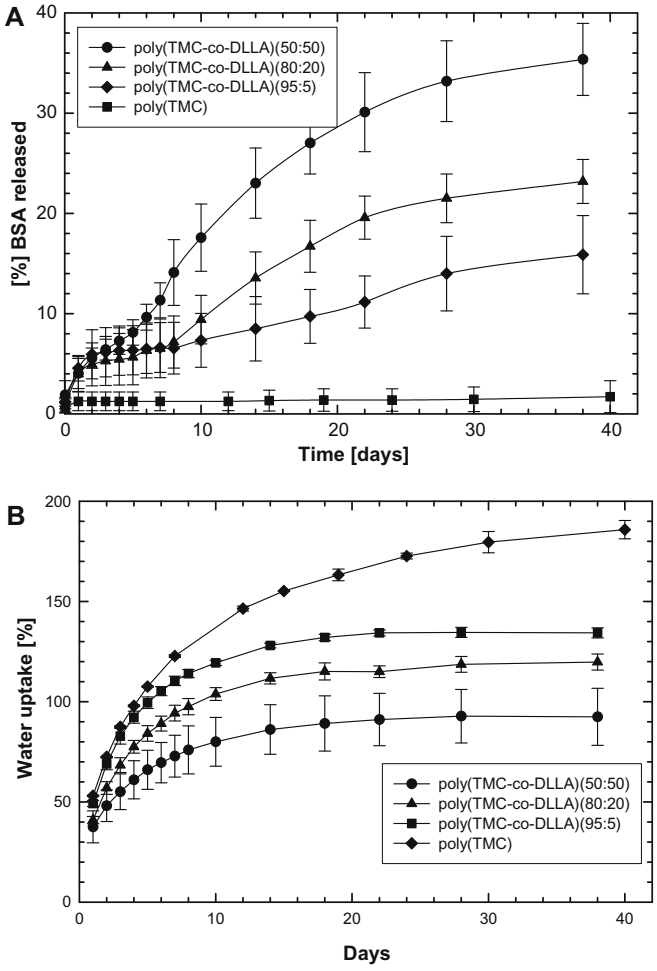

Fig. 5. (A) Cumulative mass fraction of BSA released from poly(TMC) and poly(TMC-co-DLLA) elastomeric rods, loaded with 25% by mass solid particles made of 10% BSA and 90% trehalose. (B) Percentage water uptake into poly(TMC) and poly(TMC-co-DLLA) elastomeric rods loaded with 25% by mass solid particles. The data represent the average of triplicate samples and the error bars the standard deviation about the average value.

35.4 ± 3.6%, poly(TMC-co-DLLA)(80:20) released 23.2 ± 2.2%, and poly(TMC-co-DLLA)(95:5) released 15.9 ± 3.9% of the encapsulated BSA. The lag between the first and second release periods is attributed to the time required for sufficient amounts of water to be imbibed to generate enough pressure to induce cracking within the elastomer and thus initiate release. This time period decreased as the DLLA content of the elastomer increased. Thus, the strain at break of the elastomer plays a dominant role in determining the osmotic release behavior of particles with similar osmotic and physical properties.

These results are explained mathematically as follows. Water imbibition into a capsule is described by the following equation [13,33]:

$$\frac{dV}{dt} = \frac{k_w A(\Pi - p)}{h} \tag{5}$$

where V is the amount of water imbibed, h is the capsule wall thickness, k_w is the hydraulic permeability of the polymer, A is the capsule surface area, Π is the osmotic pressure of solid particle solution in the capsule, and p is the resisting pressure of the polymer expressed as [13],

$$p = \frac{E}{6}\left(5 - \frac{4}{\lambda} - \frac{1}{\lambda^4}\right) \tag{6}$$

where E is the modulus, and λ is the ratio of the swollen capsule radius to the original radius. Thus, the smaller the elongation at break, the smaller λ, and the polymer has less tear resistance. Elastomers with greater resisting pressure require higher osmotic pressure in the capsule to rupture, because the crack formation occurs only when Π is larger than p. Thus, elastomers with greater expandability draw in larger amounts of water before being ruptured. This explanation is supported by the water uptake rates of the different

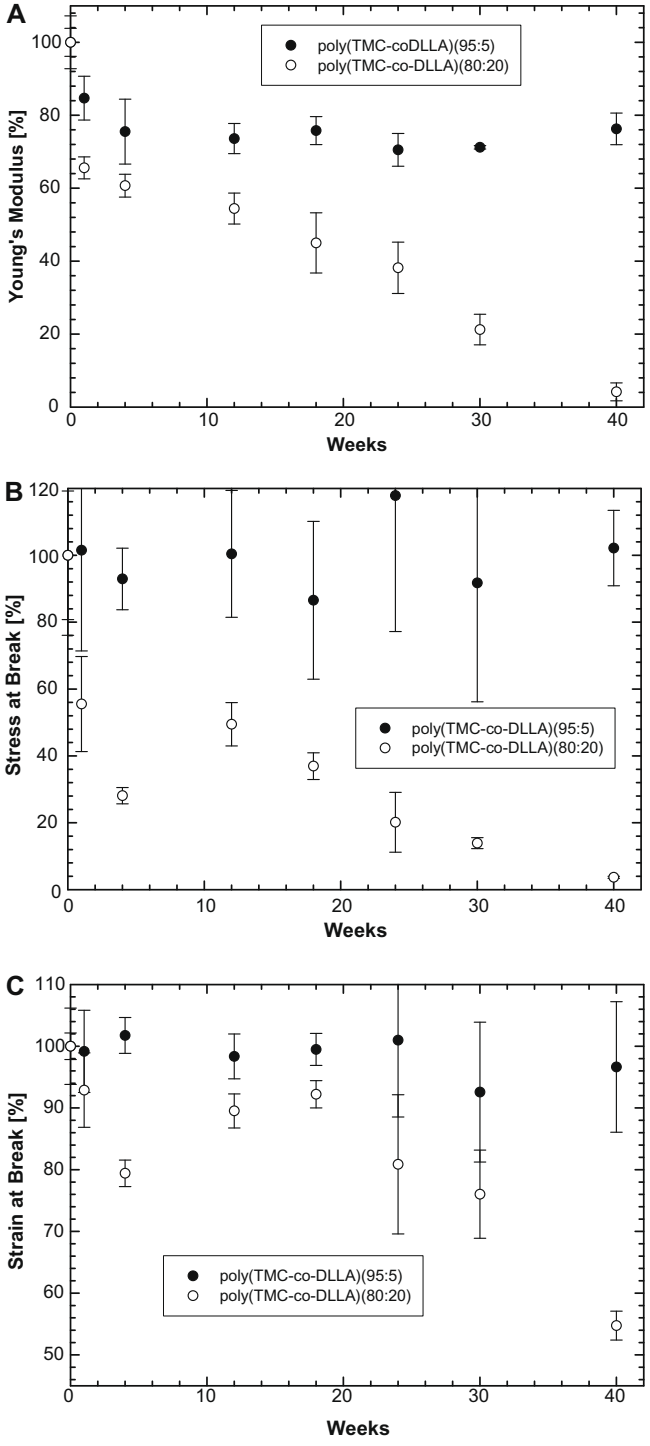

Fig. 6. Effect of *in vitro* degradation on mechanical properties of poly(TMC-co-DLLA)(80:20) elastomer (A) modulus (E), (B) ultimate tensile stress (σ_b) and (C) strain at break (ε_b). The data represent the average of triplicate samples and the error bars the standard deviation about the average value.

elastomers (Fig. 5B). Elastomers composed of solely TMC, which had the highest strain at break and lowest release rate, continually drew in water and swelled for up to 40 days in PBS buffer. Elastomers containing DLLA, on the other hand, reached an equilibrium water uptake around day 20, regardless of DLLA content.

3.5. Influence of polymer degradation

To determine the effect of the change in mechanical properties of the elastomer during the osmotic release, the hydrolytic degradation of poly(TMC-co-DLLA)(95:5) and poly(TMC-co-DLLA)(80:20) elastomers was investigated *in vitro*. Elastomers with low compositions of DLLA were chosen, since they produce fewer acidic degradation products and thus are potentially better candidates for localized delivery of acid-sensitive proteins. The changes in mechanical properties during the *in vitro* degradation are given in Fig. 6.

After a slight decrease in the modulus at week 1, poly(TMC-co-DLLA)(95:5) elastomers exhibited no change in modulus during the degradation process. The initial decrease was due to the plasticization effect of water molecules absorbed into the polymer. In the case of poly(TMC-co-DLLA)(80:20) elastomers, the modulus experienced a 34.4% decrease in its initial value at week 1, and then it decreased gradually up to week 12. After week 12, the modulus decreased at a faster rate, becoming almost immeasurable by week 40 (Fig. 6A). There was no significant difference between average modulus values from week 1 to week 12; however, the values were significantly different between week 1 and week 18, and beyond. Changes in tensile stress at break of the elastomers are shown in Fig. 6B. Similarly to the observed change in modulus, the poly(TMC-co-DLLA)(95:5) elastomer did not experience a significant change in its stress at break values during the 40 weeks of degradation. The elastomer prepared from poly(TMC-co-DLLA)(80:20), on the other hand, experienced a significant change in its stress at break values with time starting from week 30 (Fig. 6B). In contrast to the observed decrease in modulus and tensile strength with degradation time, the poly(TMC-co-DLLA)(80:20) elastomer did not experience significant alteration in its strain at break until after week 24; by week 40, the strain at break had decreased to 55% of its initial value (Fig. 6C). The poly(TMC-co-DLLA)(95:5) elastomers did not experience any drop in their strain at break values during the degradation period (Fig. 6C).

The poly(TMC-co-DLLA)(95:5) elastomer lost only 2% of its mass during the 40 weeks of investigation, and this mass loss was accompanied with a 1.3 ± 0.5% increase in sol content. In the case of the poly(TMC-co-DLLA)(80:20) elastomer, mass loss started at week 12, and by week 40, the elastomers lost 13.5 ± 1.2% of their initial mass (Fig. 7). These elastomers increasingly began to absorb water after week 12, reaching a wet mass increase of 36 ± 0.5% by week 40. This increase in water uptake was accompanied with an increase in the sol content, which reached 62 ± 8% at week 40. It can be concluded from these results that there is little influence of changes in mechanical properties of the elastomers due to degradation on the BSA release behavior, as they do not change appreciably over the release time frame.

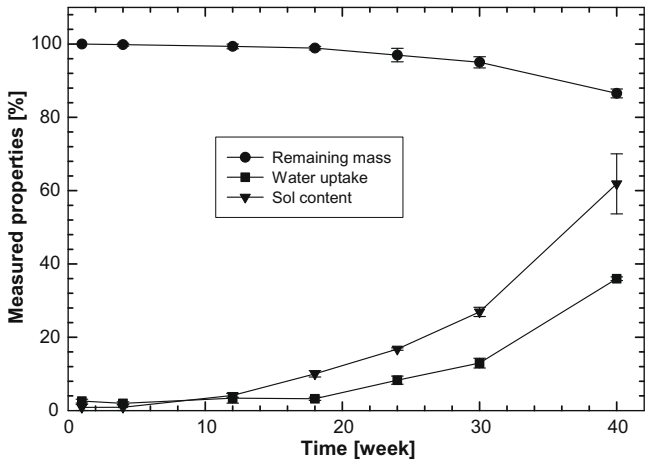

Fig. 7. Change in water uptake, sol content and mass loss of poly(TMC-co-DLLA)(80:20) elastomer during *in vitro* degradation in PBS buffer. The data represent the average of triplicate samples and error bars the standard deviation about the average value.

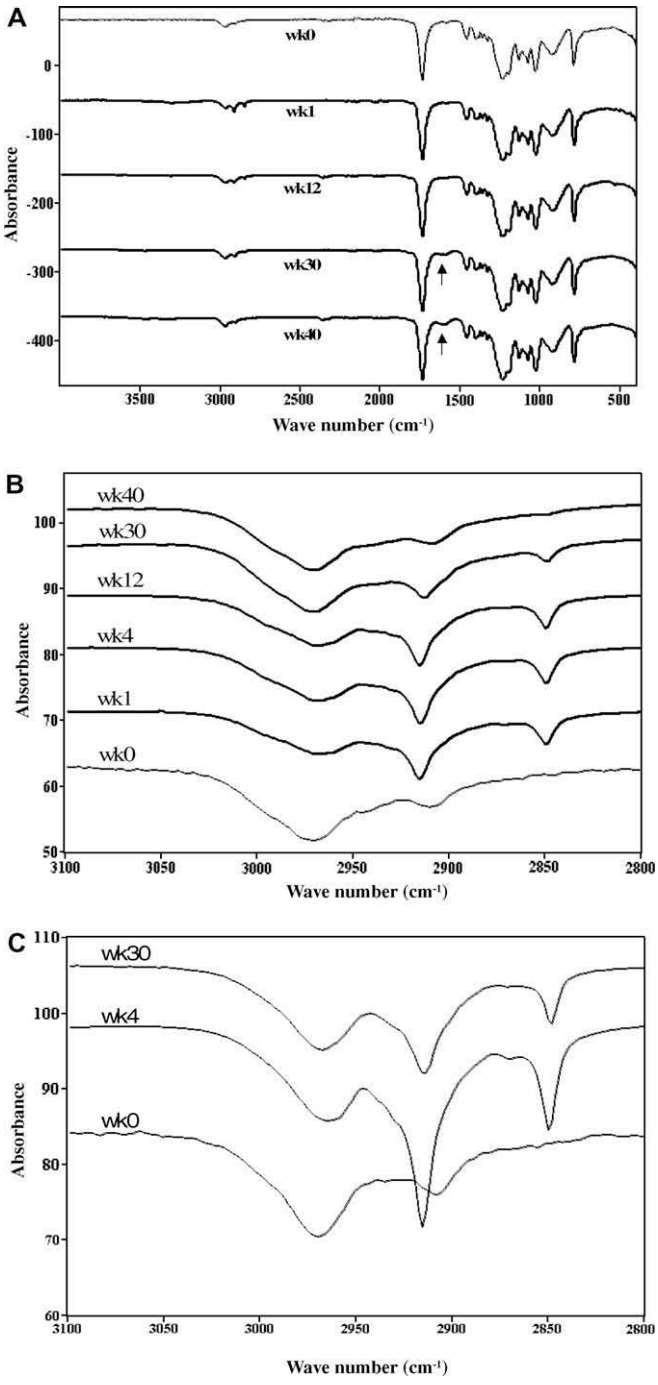

Fig. 8. ATR-FTIR analyses of *in vitro* degraded poly(TMC-co-DLLA)(80:20) elastomer. (A) Changes in the entire region. (B) Changes in the CH stretch region in the *in vitro* degraded poly(TMC-co-DLLA)(80:20) elastomer. (C) Changes in the CH stretch region in the *in vitro* degraded poly(TMC) elastomer. Arrows point to carboxylate ion peaks.

To confirm that the drop in mechanical properties at week 1 was due to plasticization effects and not to hydrolysis, and to investigate the structure of the degraded elastomer, the chemistry of the surface of degraded poly(TMC-co-DLLA)(80:20) was measured using ATR-FTIR (Fig. 8). The band at 1750 cm^{-1} was assigned to C=O stretching, the bands at 2970 cm^{-1} and 2908 cm^{-1} were due to the symmetric and asymmetric CH stretch in methine groups of TMC and in methyl and methine groups of DLLA. After immersion in buffer, the band at 2908 cm^{-1} shifted to 2916 cm^{-1} and became stronger, and a new band was formed at 2850 cm^{-1}. These bands were present only on the outer surface and not in the cross-section. The newly formed band at 2850 cm^{-1} and the shifted band at 2916 cm^{-1} returned to their initial intensity and location with time (Fig. 8B). A possible explanation is that hydrophilic regions of the elastomer become preferentially oriented at the surface due to hydration initially [34]. When the amount of water increases in the elastomer (Fig. 7), polymeric chains at the surface reorient themselves. As a result, the intensity of bands at 2850 cm^{-1} and 2916 cm^{-1} decrease and finally disappear (Fig. 8B). A similar phenomenon occurred in the hydrated poly(TMC) elastomer, known to degrade very slowly by hydrolysis (Fig. 8C) [17]. Thus, the formation of bands at 2850 cm^{-1} and 2916 cm^{-1} and the decrease in their intensity are due to surface chain orientation and are not due to degradation. At week 30 of the *in vitro* degradation, a band appeared at 1600 cm^{-1}, due to the formation of carboxylate ion in the degraded elastomer (Fig. 8A). The intensity of the band at 1600 cm^{-1} became stronger at week 40 as the degradation progressed. The ATR-FTIR results do not show any significant degradation at week 1, thus changes in mechanical properties at week 1 are primarily due to the absorption of water.

3.6. Microenvironmental pH

The rate of DLLA hydrolysis is slow, and so it was reasoned that there would be little change in the microenvironmental pH within the interior of the elastomer during degradation. To test this hypothesis, and to investigate why the total release of the particles was low, FITC-BSA was lyophilized with trehalose under the same conditions as BSA, and these particles were loaded into poly(TMC-co-DLLA)(80:20). The FITC-BSA-loaded elastomer was imaged at depths of up to 160 μm, prior to (Fig. 9A) and after (Fig. 9B) 17 days

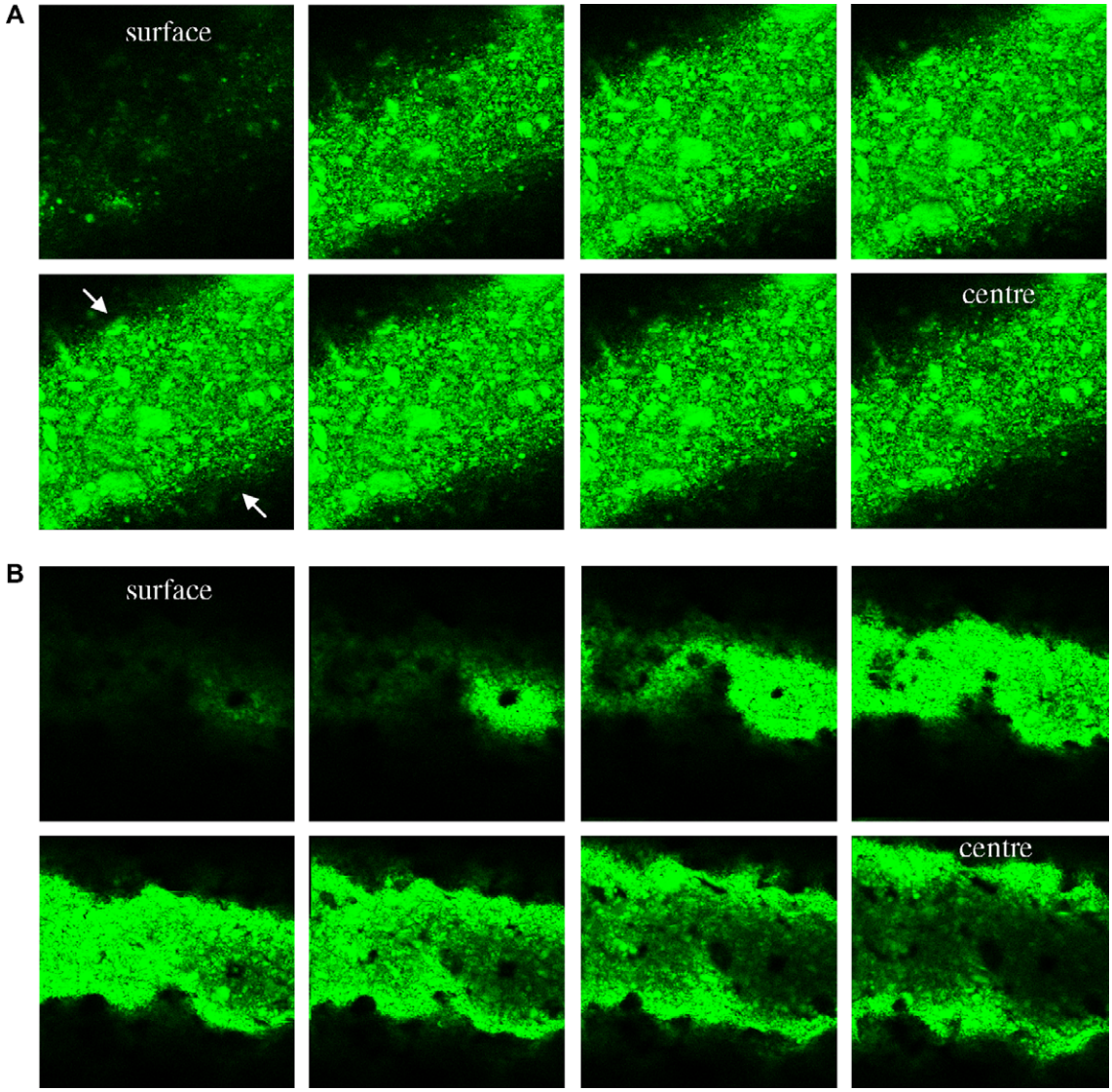

Fig. 9. (A) Images of particles of FITC-BSA co-lyophilized with trehalose embedded in the in poly(TMC-co-DLLA)(80:20) elastomer rods before immersion in buffer. The outer boundaries are indicated by the arrows. (B) Images of the particles after 17 days of release in PBS buffer. The images were taken in the radial direction towards the centre of the rod at 20 μm intervals, and the particle loading was 25% by mass. (For interpretation to colours in this figure, the reader is referred to the web version of this paper.)

of release, via laser scanning confocal microscopy. The results show that the FITC-BSA particles maintained their fluorescence after 17 days. As FITC no longer fluoresces below pH 5, it can be concluded that the internal pH did not drop significantly. From the images, it is apparent that particle release occurs from surface regions of the rods and progresses into the centre with time, in accordance with the osmotic release mechanism. However, by 17 days, when release had almost ceased, only those particles in the outer region of the rod were released. This is likely due to an insufficient water activity gradient being formed between the water in the outer region of the rod containing unreleased trehalose and BSA in the microcracks formed, and the water contacting encapsulated particles in the inner regions of the rod.

3.7. Influence of particle loading

To examine the effect of the initial volumetric loading of particles on the release rate and total mass fraction of BSA released, rods of poly(TMC-co-DLLA)(80:20) with three volumetric loadings of 8.3%, 12.6% and 21.5% (corresponding to weight loadings of 10%, 15% and 25%) were prepared, and the rate of BSA release was measured. The volumetric loading did not have a large impact on the mass fraction release rate of BSA (Fig. 10A). The rate of release was slightly greater initially in the case of lower volumetric loadings, but beyond day 4, the release rates were similar. The water uptake, however, was three times greater when the loading was 25% compared to 10% loading (Fig. 10B). Elevated amounts of water in the device could potentially denature unreleased protein therapeutics. Therefore, since the volumetric loading does not have significant impact on the rate and total mass fraction of BSA released, provided the loading is below the critical loading, it is advisable to use lower volumetric loadings.

The release of BSA was incomplete over the time frame studied in the formulations investigated. This was likely due to the presence of stable, swollen particle capsules within the interior of the rods, which result when the osmotic pressure difference between the solutions formed within the capsule is insufficient to generate microcracks within the elastomer bulk as illustrated in Ref. [12] and in Fig. 9B. The remaining protein would require the degradation of the elastomer matrix to be released.

3.8. Influence of increasing osmotic activity of particle

In an effort to increase the osmotic activity of the encapsulated solid excipient, BSA was lyophilized with a mixture of trehalose and NaCl. As noted earlier, a saturated solution of trehalose has an osmotic pressure of 92 atm, while a saturated solution of NaCl can provide an osmotic pressure of 345 atm at 37 °C [6]. The effect

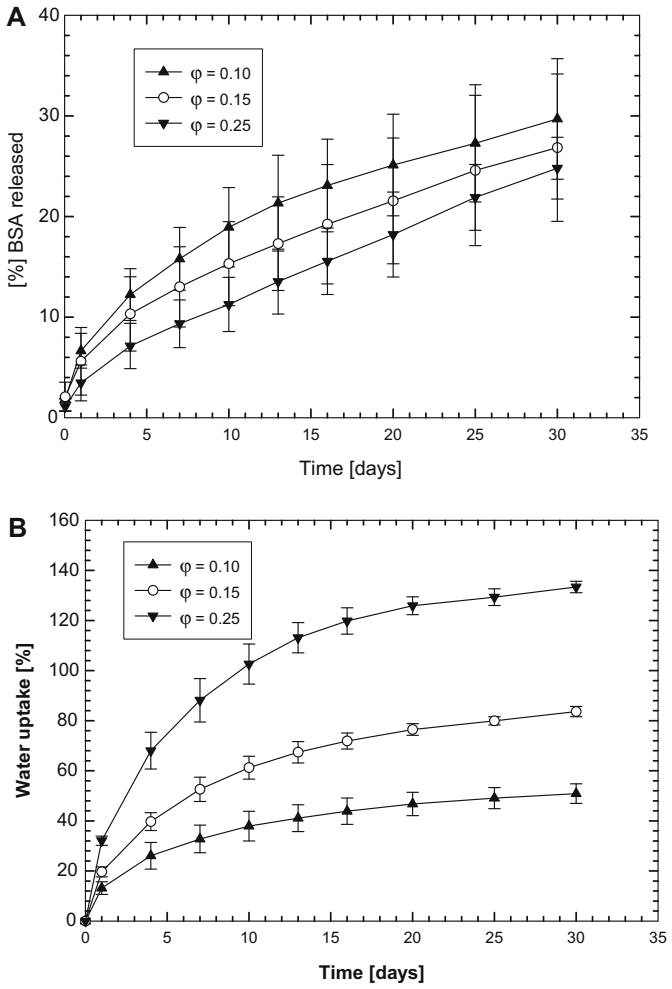

Fig. 10. (A) Effect of particle loading on the cumulative mass fraction release of BSA from poly(TMC-co-DLLA)(80:20) elastomer rods. (B) Percentage water uptake into the poly(TMC-co-DLLA)(80:20) elastomer rods at different particle loadings. φ represents the mass fraction of particles initially loaded into the rods.

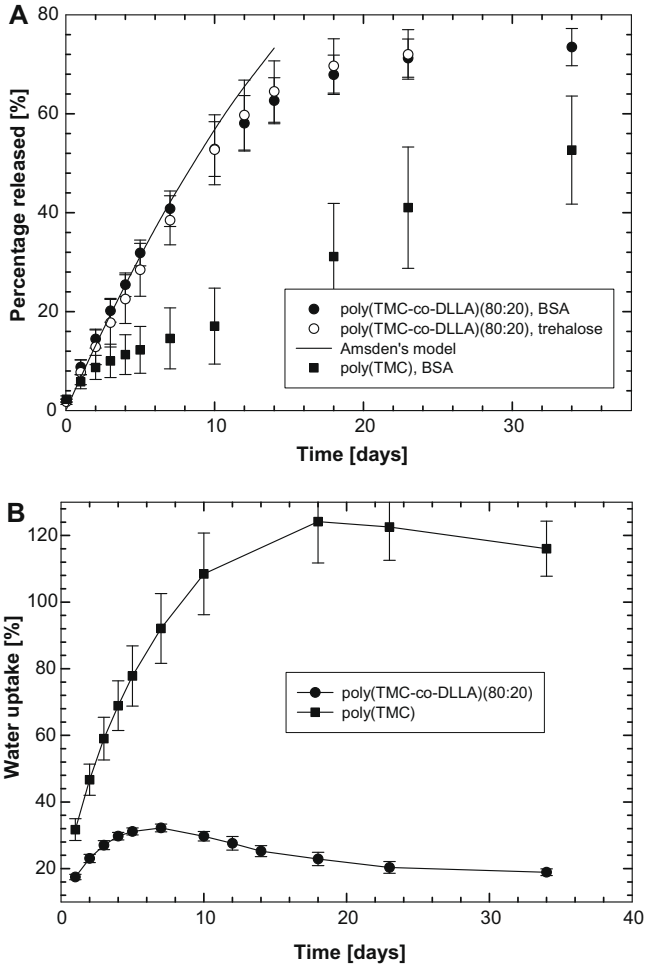

Fig. 11. (A) Cumulative mass fraction of BSA and trehalose release from poly(TMC) and poly(TMC-co-DLLA)(80:20) elastomeric rods, loaded with 10% by mass of solid particles made of 10% BSA, 25% NaCl and 65% trehalose. (B) Percentage water uptake into poly(TMC) and poly(TMC-co-DLLA) elastomeric rods loaded with 10% by mass solid particles. The data represent the average of triplicate samples and the error bars the standard deviation about the average value.

of increasing the osmotic pressure within the swelling particle capsule was dependent on the nature of the elastomer. Increasing the osmotic pressure of the solution generated by dissolution of the solid excipient had a minor effect on providing an effective release from the TMC elastomer (Fig. 11A). For these rods, the cumulative release of BSA was 17.1 ± 7.7% at day 10, the rate of release increased after day 10 reaching 52.6 ± 10.9% at day 34, and the increase in the rate of release was accompanied with a decrease in water uptake (Fig. 11B). By contrast, increasing the osmotic pressure of encapsulated solid particles increased both the release rate and total amount of BSA release from poly(TMC-co-DLLA)(80:20). The release was approximately zero order for a period of 12 days and was sustained for a period of 34 days. The total amount of BSA released was 73.5 ± 3.8% after 34 days (Fig. 11A). Moreover, both BSA and trehalose were released at similar rates, as has been found previously [4,16]. The water uptake profile in this system exhibited a maximum at day 7, after which it decreased (Fig. 11B). This result supports the conclusion that effective osmotic release occurs at low values of water uptake.

The following equation [13] for osmotic pressure driven release from cylindrical rubbery non-degradable polymer matrices was fitted to experimental data to evaluate the time required for a capsule layer to burst (t_b),

$$\frac{m_t}{m_T} = \frac{1}{1+\frac{\bar{R}}{x}}\left[\left(2+\frac{x}{R}\right)\left(\frac{t}{t_b}-\frac{x}{R}\left(\frac{t}{t_b}\right)^2\right)\right] \tag{7}$$

where m_t/m_T is the mass fraction of drug released, x is the thickness of the particle layer, t is the time, and R is the diameter of the cylindrical device. Particle layers were assumed to have the structure of a concentric cannuli. The thickness of the particle layer was calculated from $x = \bar{h} + 2r_0$, in which $\bar{h}$ could be evaluated using the following equation:

$$\bar{h} = \frac{L - nd}{n+1} \tag{8}$$

in which L is the length of a cube matrix, which has an equivalent volume to a cylindrical device, and n is the number of solid particles in the device. The parameter n is calculated from the following equation:

$$n = \frac{L}{d}\phi^{\frac{1}{3}} \tag{9}$$

in which ϕ is the volumetric loading, and d is the diameter of solid particles. The average diameter of the device was 1.54 ± 0.01 mm, the average length was 12.56 ± 0.18 mm, and the average radius of solid particles was 78.7 ± 21.2 μm. The area of solid particles, which had a non-circular shape, was measured using Motic Images Plus 2 software, and the radius of a circle with an equivalent area was calculated. The density of solid particles was taken as 1.587 g cm^{-3} based on the density of its components. The density of the elastomer was 1.281 g cm^{-3} (Table 2), and the volumetric loading was 7.7%. Based on these numbers, the average thickness of the particle layer was calculated to be 345.7 μm. By fitting the model to experimental data using a least squares approach, t_b was found to be 11.2 ± 2.4 days (R^2 = 0.989). The time to burst is proportional to the square of the particle size according to the following equation [13]:

$$t_b = \frac{r_0^2}{k_w}\int_1^{\lambda_c} \frac{\left[\left[\lambda^3 + \left(\frac{\bar{h}}{r_0}+1\right)^3 - 1\right]^{1/3} - \lambda\right]}{(\pi - p)} d\lambda \tag{10}$$

where r_0 is the radius of the particle, and λ_c is the ultimate radial extension of the swollen capsule. Thus, larger particles result in a greater time to burst. The model provides a very good fit to the experimental data, especially for the initial 12 days (Fig. 11A). The model does not provide an adequate representation of the release at later stages. This is most probably due to longer times required for the drug to be forced out of the device when the polymer cracking activity extends deep towards the centre of the cylinder.

4. Conclusions

Poly(TMC-co-DLLA) elastomers with low-DLLA content have a higher potential of success than poly(DLLA-co-CL)(50:50) elastomers, investigated previously [8,15], for the localized delivery of acid labile proteins via an osmotic release mechanism. This is due to two reasons: the first is that lower content of DLLA generates less acid degradation products, and acid auto-catalyzed degradation stage will proceed at a slower rate compared to the poly(DLLA-co-CL)(50:50) elastomer. The second reason is that unlike the ester groups of ε-CL [35], the carbonate groups of the TMC chains undergo very little hydrolysis even at pH values as low as 2 [19]. The *in vitro* degradation study indicated that degradation played a minor role in the osmotic release, since mechanical properties undergo very little change during the investigated period of release. Elongation at break plays a dominant role in determining osmotic release behavior when the device is elastic and embedded particles have sufficient osmotic activity to rupture the elastomer. To improve osmotic release capabilities, TMC was copolymerized with DLLA. The incorporation of small amounts of DLLA decreased the tear resistance of the elastomer and improved the osmotic release of the incorporated protein. The poly(TMC-co-DLLA)(80:20) elastomer was able to provide a near zero order release of BSA for up to 12 days, and the total amount of BSA released was 74 ± 4% after 34 days. The degradation results indicate that TMC elastomers copolymerized with small amounts of DLLA degrade slowly with no significant reduction in the microenvironmental pH.

Acknowledgements

The authors would like to acknowledge funding provided by the Canadian Institutes of Health Research. Rafi Chapanian was the recipient of an Ontario Graduate Scholarship for Science and Technology.

References

[1] B. Amsden, Review of osmotic pressure driven release of proteins from monolithic devices, Journal of Pharmacy and Pharmaceutical Sciences 10 (2) (2007) 129–143.
[2] R.A. Siegel, J. Kost, R. Langer, Mechanistic studies of macromolecular drug release from macroporous polymers. 1. Experiments and preliminary theory concerning completeness of drug release, Journal of Controlled Release 8 (3) (1989) 223–236.
[3] S. Frokjaer, Biomaterials for Delivery and Targeting of Proteins and Nucleic Acids, CRC Press, 2005.
[4] B. Amsden, Y.L. Cheng, A generic protein delivery system based on osmotically rupturable monoliths, Journal of Controlled Release 33 (1) (1995) 99–105.
[5] V. Carelli, G. Dicolo, C. Guerrini, E. Nannipieri, Drug release from silicone elastomer through controlled polymer cracking – an extension to macromolecular drugs, International Journal of Pharmaceutics 50 (3) (1989) 181–188.
[6] R. Gale, S.K. Chandrasekaran, D. Swanson, J. Wright, Use of osmotically active therapeutic agents in monolithic systems, Journal of Membrane Science 7 (3) (1980) 319–331.
[7] F. Gu, B. Amsden, R. Neufeld, Sustained delivery of vascular endothelial growth factor with alginate beads, Journal of Controlled Release 96 (3) (2004) 463–472.
[8] F. Gu, R. Neufeld, B. Amsden, Sustained release of bioactive therapeutic proteins from a biodegradable elastomeric device, Journal of Controlled Release 117 (1) (2007) 80–89.
[9] R.F. Fedors, Osmotic effects in water-absorption by polymers, Polymer 21 (2) (1980) 207–212.
[10] P.D. Riggs, P. Kinchesh, M. Braden, M.P. Patel, Nuclear magnetic imaging of an osmotic water uptake and delivery process, Biomaterials 22 (5) (2001) 419–427.

[11] R. Schirrer, P. Thepin, G. Torres, Water-absorption, swelling, rupture and salt release in salt silicone-rubber compounds, Journal of Materials Science 27 (13) (1992) 3424–3434.
[12] B.G. Amsden, Y.L. Cheng, Enhanced fraction releasable above percolation-threshold from monoliths containing osmotic excipients, Journal of Controlled Release 31 (1) (1994) 21–32.
[13] B. Amsden, A model for osmotic pressure driven release from cylindrical rubbery polymer matrices, Journal of Controlled Release 93 (3) (2003) 249–258.
[14] B.G. Amsden, Y.L. Cheng, M.F.A. Goosen, A mechanistic study of the release of osmotic agents from polymeric monoliths, Journal of Controlled Release 30 (1) (1994) 45–56.
[15] F. Gu, R. Neufeld, B. Amsden, Osmotic-driven release kinetics of bioactive therapeutic proteins from a biodegradable elastomer are linear, constant, similar, and adjustable, Pharmaceutical Research 23 (4) (2006) 782–789.
[16] F. Gu, H.M. Younes, A.O.S. El-Kadi, R.J. Neufeld, B.G. Amsden, Sustained interferon-gamma delivery from a photocrosslinked biodegradable elastomer, Journal of Controlled Release 102 (3) (2005) 607–617.
[17] R. Chapanian, M.Y. Tse, S.C. Pang, B.G. Amsden, The role of oxidation and enzymatic hydrolysis on the in vivo degradation of trimethylene carbonate based photocrosslinkable elastomers, Biomaterials 30 (3) (2009) 295–306.
[18] G.H. Stoll, F. Nimmerfall, M. Acemoglu, D. Bodmer, S. Bantle, I. Muller, A. Mahl, M. Kolopp, K. Tullberg, Poly(ethylene carbonate)s, part II: degradation mechanisms and parenteral delivery of bioactive agents, Journal of Controlled Release 76 (3) (2001) 209–225.
[19] Z. Zhang, R. Kuijer, S.K. Bulstra, D.W. Grijpma, J. Feijen, The in vivo and in vitro degradation behavior of poly(trimethylene carbonate), Biomaterials 27 (9) (2006) 1741–1748.
[20] B.G. Amsden, M.Y. Tse, N.D. Turner, D.K. Knight, S.C. Pang, In vivo degradation behavior of photo-cross-linked star-poly(epsilon-caprolactone-co-D,L-lactide) elastomers, Biomacromolecules 7 (1) (2006) 365–372.
[21] B.G. Amsden, G. Misra, F. Gu, H.M. Younes, Synthesis and characterization of a photo-cross-linked biodegradable elastomer, Biomacromolecules 5 (6) (2004) 2479–2486.
[22] M.M. Bradford, Rapid and sensitive method for quantitation of microgram quantities of protein utilizing principle of protein–dye binding, Analytical Biochemistry 72 (1–2) (1976) 248–254.
[23] M. Dubois, K.A. Gilles, J.K. Hamilton, P.A. Rebers, F. Smith, Colorimetric method for determination of sugars and related substances, Analytical Chemistry 28 (3) (1956) 350–356.
[24] C. Jie, K.J. Zhu, Preparation, characterization and biodegradable characteristics of poly(D,L-lactide-co-1,3-trimethylene carbonate), Polymer International 42 (4) (1997) 373–379.
[25] R.F. Storey, S.C. Warren, C.J. Allison, A.D. Puckett, Methacrylate-endcapped poly(D,L-lactide-co-trimethylene carbonate) oligomers. Network formation by thermal free-radical curing, Polymer 38 (26) (1997) 6295–6301.
[26] S.M. Li, J.L. Espartero, P. Foch, M. Vert, Structural characterization and hydrolytic degradation of a Zn metal initiated copolymer of L-lactide and epsilon-caprolactone, Journal of Biomaterials Science-Polymer Edition 8 (3) (1996) 165–187.
[27] R. Yamadera, M. Murano, Determination of randomness in copolyesters by high resolution nuclear magnetic resonance, Journal of Polymer Science Part A-1: Polymer Chemistry 5 (9PA1) (1967) 2259–2268.
[28] A.P. Pego, A.A. Poot, D.W. Grijpma, J. Feijen, Physical properties of high molecular weight 1,3-trimethylene carbonate and D,L-lactide copolymers, Journal of Materials Science: Materials in Medicine 14 (9) (2003) 767–773.
[29] A.C. Albertsson, M. Eklund, Influence of molecular-structure on the degradation mechanism of degradable polymers – in-vitro degradation of poly(trimethylene carbonate), poly(trimethylene carbonate-co-caprolactone), and poly(adipic anhydride), Journal of Applied Polymer Science 57 (1) (1995) 87–103.
[30] R. Chapanian, Long term in vivo degradation, and tissue response to, photo-cross-linked elastomers prepared from star shaped prepolymers of poly(e-caprolactone-co-D,L-lactide), Journal of Biomedical Materials Research Part A (2009), doi:10.1002/jbm.a.32422.
[31] J.K. Kaushik, R. Bhat, Why is trehalose an exceptional protein stabilizer? An analysis of the thermal stability of proteins in the presence of the compatible osmolyte trehalose, Journal of Biological Chemistry 278 (29) (2003) 26458–26465.
[32] S. Sharifpoor, B. Amsden, In vitro release of a water-soluble agent from low viscosity biodegradable, injectable oligomers, European Journal of Pharmaceutics and Biopharmaceutics 65 (3) (2007) 336–345.
[33] F. Theeuwes, Elementary osmotic pump, Journal of Pharmaceutical Sciences 64 (12) (1975) 1987–1991.
[34] N.T. Paragkumar, E. Dellacherie, J.L. Six, Surface characteristics of PLA and PLGA films, Applied Surface Science 253 (5) (2006) 2758–2764.
[35] H. Kweon, M.K. Yoo, I.K. Park, T.H. Kim, H.C. Lee, H.S. Lee, J.S. Oh, T. Akaike, C.S. Cho, A novel degradable polycaprolactone networks for tissue engineering, Biomaterials 24 (5) (2003) 801–808.